

A COMPARATIVE STUDY OF SHALE PORE STRUCTURE ANALYSIS

R. Cicha-Szot, P. Budak, G. Leśniak, P. Such,
Instytut Nafty i Gazu - Państwowy Instytut Badawczy, Kraków, Poland

This paper was prepared for presentation at the International Symposium of the Society of Core Analysts held in Vienna, Austria, 27 August -1 September 2017

ABSTRACT

One of the challenges of economically exploiting shale gas reservoirs is proper estimation of gas flow rate. To achieve this goal, better understanding of pore structure and flow paths in fine grained rocks is needed. The nano to micrometer scales of pore systems requires more complex analysis and application of different techniques to understand pore changes in shale systems. Except for pore size analysis using scanning electron microscopy, in this study mercury intrusion capillary pressure (MICP), nitrogen adsorption and Klinkenberg gas slippage analysis are considered to evaluate pore size. Gas slippage measures the pores most responsible for fluid flow and can be applied at levels of stress comparable to those experienced during reservoir production. However, pore size and pressure restricts the slippage effect, which is not visible in every rock. In this study, slippage was measured on plugs oriented parallel to bedding. All samples were pre-stressed at reservoir conditions ($\sigma_{\text{eff}} \sim 33$ MPa). Due to the high heterogeneity of the analyzed shale samples, Klinkenberg permeability, SEM, MICP and nitrogen adsorption analysis were performed on the same plug to obtain the most adequate and coherent pore size results.

Theoretical calculations of average pore diameter derived from slippage data collected in this study for samples with high clay content and low carbonate content yielded lower diameters than estimates from MICP data. Pore size evaluated with MICP and Klinkenberg gave similar results for samples with existing microfractures. Although similar pore diameters might be distinguished on SEM images, detailed pore size analysis using FIB-SEM showed very different results when evaluated with gas slippage.

INTRODUCTION

Permeability is one of the parameters in the evaluation of shale play and the finding of production sweet spots. Pore space geometry and mineral composition influence hydrocarbon production through wettability, capillarity and all phenomena which may occur in nanometer scale pores such as diffusion, condensation etc. [1]. Moreover, fluid flow in shales occurs not only in the mineral matrix, but also in connected organic matter and in natural and induced microfractures. The latter are crucial in estimating permeability because they provide less resistance to flow than nano-sized pores. In recent years, several physical flow models have been proposed to estimate shale permeability; however, all these models require effective pore diameter as an input parameter. Techniques applied to characterize pore systems in conventional reservoir rocks such as mercury intrusion, low pressure gas adsorption or scanning electron microscopy may provide general information

about pore size distribution in shales; however, because of shale ductility and different stress conditions, it might not be sufficient to adequately characterizing pore systems in shales. Moreover, the high pressures applied during mercury intrusion capillary pressure analysis may alter nanopore space.

Slippage measurements for analyzing shale pore structures make it possible to obtain pore sizes in stressed samples. Moreover, such a technique characterizes only the part of the pore system that is responsible for fluid flow. Very few studies have been published that include gas slippage measurement on stressed shale samples [2,3]; however, these studies were performed on mudstones or siltstones, whereas Central European shale formations are mainly claystones, which are more prone to deformation of pore space with effective stress.

In this study, stress-dependent unsteady-state gas permeability measurements were performed. Analysis of Klinkenberg gas slippage effect in comparison with other pore structure characterization techniques is presented.

SAMPLES AND METHODS

The comparison of pore structure analysis was conducted using a series of 10 samples with different fabrics and compositions which represent silurian and ordovician shale formations from the Baltic Basin. The average mineralogical composition of these shale samples is: quartz (21.6 – 43.2 %), minerals from the illite muskovite group (25.9 – 37.75 %), carbonate represented by calcite, dolomite and ankerite (25.9 – 37.8 %), chlorites (3.7 – 13.2 %), plagioclase (2.7 – 5.8%), feldspar (0.7 – 5.2 %), minerals from the illite/smectite group (1.2-7.7%). Mineral composition of samples determined by X-ray diffraction (XRD) is shown in Table 1.

Table 1. Mineral composition of selected samples

Sample ID	Quartz	Total carbonate	Total clay	Pl	F-K	P	Mr
	[%]	[%]	[%]	[%]	[%]	[%]	[%]
3	25.1	16.3	47.0	5.1	2.1	4.4	-
8	21.6	18.1	47.8	4.4	1.5	4.2	2.4
11	23.4	1.3	57.5	4.6	0.9	7.9	3.6
14	25.4	1.4	60.9	5.8	1.9	3.0	1.6
19	28.4	7.1	51.9	4.3	2.5	4.2	1.7
29	26.9	10.7	54.4	3.2	1.7	2.6	0.5
32	34.8	1.8	46.3	5.2	5.2	5.2	1.5
42	26.7	3.1	57.6	4.0	3.2	3.0	2.4
47	31.4	2.8	51.6	4.2	2.9	5.5	1.6
48	29.0	1.8	57.7	4.1	2.7	3.4	1.3

Pl-plagioclase, F-K – potassium feldspar, C- carbonates, P – pyrite, Mr- marcasite,

Stress-dependent unsteady state nitrogen permeability measurements were performed on 1-inch diameter plugs using the pressure pulse decay method. Plugs were run at a range of simple effective stresses defined as the difference between confining pressure and pore pressure. All samples were tested at an effective stress of 33MPa, which imitates reservoir conditions of shale formations in the Baltic Basin. Additionally, to determine the impact

of pore pressure decrease on effective pore diameter, two samples (32 and 42) were subjected to stress of 4.8, 8.2 and 19.9 MPa. The samples were left for 24 hours at each new simple effective stress to allow them to equilibrate at the new stress condition. Klinkenberg plots were generated by plotting permeability versus the inverse of mean pore pressure. Derived from the slope of linear fit of permeability vs inverted pore pressure crossplot, Klinkenberg's slippage parameter was used to calculate pore size assuming slit-shaped and tube-shaped pores.

Prior to permeability testing, the plugs were imaged with a micro X-ray CT scanner and radiography to characterize density and distribution of fractures and distinguish laminations which may affect permeability. In turn, after the permeability measurements, the plugs were crushed and destructive analyses were performed including petrographic analysis (on polished thin sections), scanning electron microscopy (SEM and FIB-SEM), mercury intrusion, low-pressure adsorption, XRD and Rock-Eval analysis.

Petrographic analyses of thin sections and SEM analyses of ion polished sections were performed on mirrored surfaces of the plug (circular cross-section) to characterize the structure and texture of the analyzed shale samples as well as the distribution of natural and induced microfractures. SEM analysis was conducted on a Helios NanoLab 450HP (FEI).

For comparison with pore size obtained by slippage measurements, pore structures were characterized by mercury intrusion (MICP) with Micromeritics AutoPore IV and low pressure nitrogen adsorption at 77K using a TRISTAR apparatus. Pore size distributions were calculated from adsorption data using the Barrett, Joyner, Halenda (BJH) method and FAAS correction.

This experimental program minimized the effect of heterogeneity of shale formation, thus providing more comparable data.

Table 2 Porosity, surface area, TOC and permeability of samples analyzed in this study

Sample ID	Total porosity*	Open porosity*	Specific	BET	TOC	Permeability
	[%]		surface area	surface area**		
	[%]	[%]	[m ² /g]	[m ² /g]	[%]	10 ⁻¹⁵ [m ²]
3	13.15	1.64	1.65	10.56	0.96	0.004075
8	11.16	3.03	2.84	13.02	1.19	0.000605
11	14.59	3.59	1.56	7.96	1.98	0.025966
14	16.12	0.48	0.17	7.67	2.15	0.000584
19	14.57	1.81	2.01	5.63	1.8	0.005894
29	18.57	1.65	1.71	10.98	0.57	0.001971
32	16.20	5.27	5.15	5.84	1.62	0.031097
42	12.59	3.95	2.32	4.32	4.5	0.104597
47	13.16	3.72	4.15	6.46	3.54	0.000358
48	14.98	0.94	0.68	3.27	3.7	0.000228

*unstressed porosity; ** from N₂ adsorption data

RESULTS AND DISCUSSION

Complex non-destructive characterization of samples prior to permeability measurements is crucial to estimate the matrix permeability of shale samples [4]. Micro X-ray computed tomography (MXCT) and radiography showed a network of natural and/or induced microfractures (image resolution $\sim 6\mu\text{m}$) in all analyzed samples. In most cases, the microfractures are not parallel to lamination or are partially filled with pyrite or calcite, which suggests a natural origin of such microfractures (MXCT image of sample 14 and 42 - Table 3). Moreover, in samples 11 and 14 laminations with thicker detrital material can be distinguished. None of the distinguished microfractures runs through whole sample length (length of the samples is ca. 2.3 inches), thus flow-through the samples is affected by the effective pore throats of the matrix. The samples show different structures and, as a result, various pore space geometries; for example, samples 3 and 8 can be classified as clayey-silt micro heterolites (Table 4).

Table 3 MXCT and RTG images of investigated core samples (Part 1)

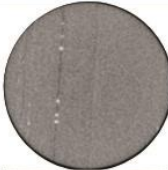
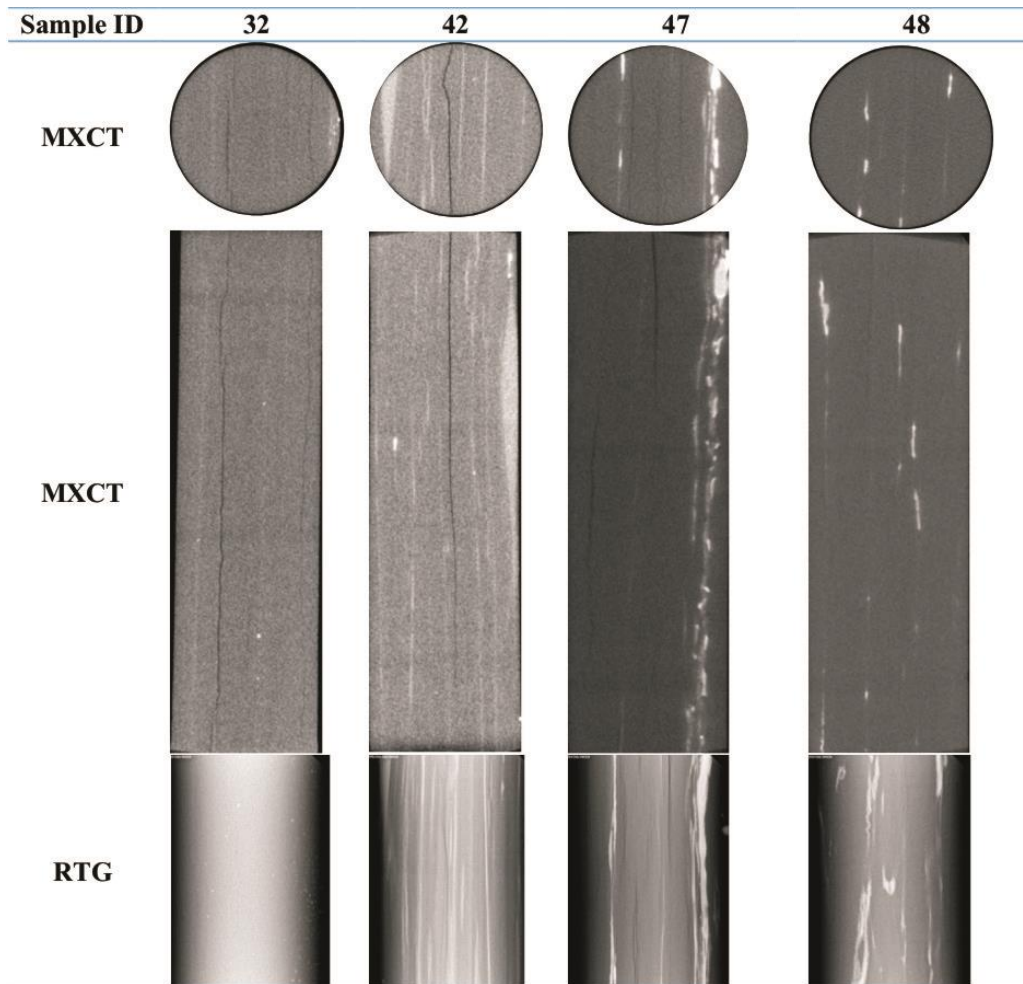
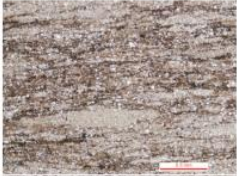
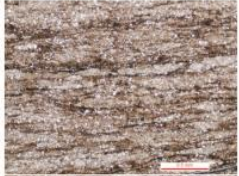
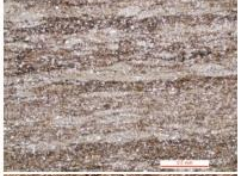
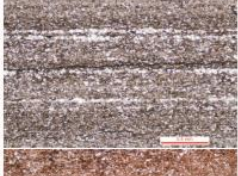
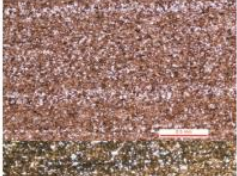
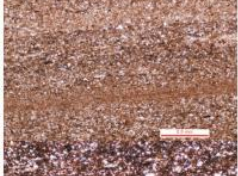
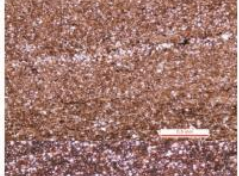
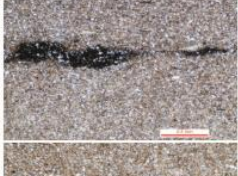
Sample ID	3	8	11	14
MXCT				
MXCT				
RTG				

Table 3 MXCT and RTG images of investigated core samples (Part 2)



Pore size distribution for each sample determined using MICP and low pressure adsorption are presented on Figure 1. For samples 11, 14, 47 and 48, effective pore diameter calculated from Klinkenberg is lower due to specific mineral composition consisting of over 50% clay content; also, 5-11% of pyrite and ca. 2% of carbonates may fill up natural microfractures. Moreover, for these samples, relatively high TOC content (2-3.7%) and permeability in the range of several hundreds of nanodarcy were observed. An exception is sample 11, which has permeability in the microdarcy range, probably due to laminations with thicker detrital material and microfractures visible on MXCT, which may affect this permeability value. The remaining samples, which have higher quartz and/or carbonate content, show Klinkenberg pore diameters similar to the dominating pore diameters from MICP or nitrogen adsorption. Such consistency of results may be related to several effects, such as less susceptibility to compression or the occurrence of a specific network of microfractures.

Table 4. Thin sections of selected shale samples

Sample ID	Thin section		
3			
8			
11			
14			
32			
42			
47			
48			

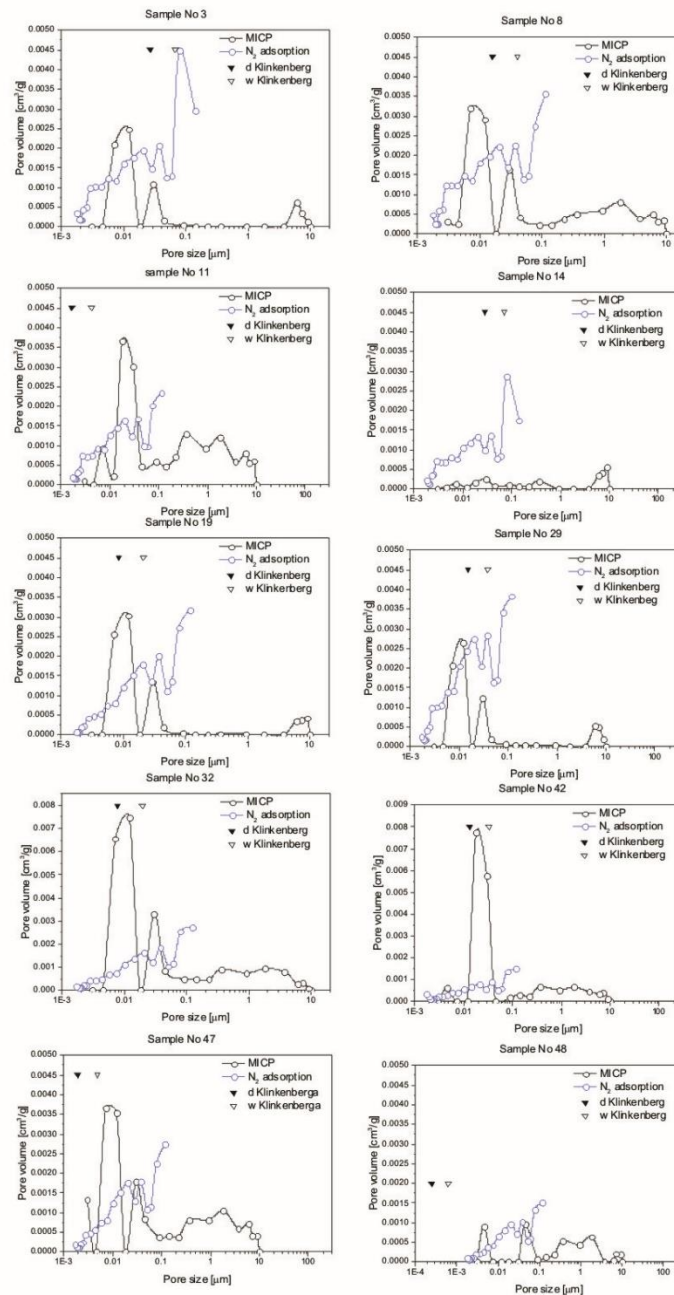


Figure 1. MICP and low pressure nitrogen adsorption data. Triangle points show pore sizes calculated according to Klinkenberg at reservoir conditions of the Baltic Basin shale formations. d – diameter of tube shaped pores, w – width of slit shaped pores.

Samples 3, 8, 19 and 29 have very similar pore size distribution curves with high content of micropores and nanopores that can be seen only with nitrogen adsorption; this may suggest deformation of pores formed from clay sheets or pores in organic matter caused by high mercury injection pressure. The most pronounced effect is seen in sample 29, which consists of 54% clay minerals and is characterized by a high BET surface area (over 10

m²/g). Generally, for samples with domination of nano sized pores observed in MICP, pore diameter at 75% mercury saturation might be assumed as the effective pore diameter that determines flow. In turn, in samples with extremely low open porosity (0.48% - sample 14), effective pore diameter is close to the dominant pore size diameter estimated from nitrogen adsorption data.

In samples 32 and 42, which have very dense low range distribution of microfractures and a bigger microfracture that is clearly seen in MXCT, similar values of Klinkenberg and MICP diameter might be due to the principles of MICP analysis, which sees microfractures as pore throats and, thus, increases the value of effective pore size diameter.

Although, microfractures and pores with diameters in the nanometer range are quite often seen on SEM images, average microfracture widths for samples 32 and 42 (calculated from SEM in an unstressed state) are 3 and 2 times wider, respectively (Table 5). Moreover, more detailed SEM analysis and calculation of average pore diameters using FIB-SEM data showed larger values; this suggests that SEM images of unstressed pores are not geometrically representative of pore structures in the subsurface and cannot be considered during permeability estimation of shale reservoirs.

Table 5 Comparison of slit-shaped pore size and tube-shaped pore size from SEM and Klinkenberg

Sample ID	Pore width Klinkenberg	Pore width SEM	Pore diameter Klinkenberg	Pore diameter FIBSEM (median)
	[m]	[m]	[m]	[m]
8	$4.05 \cdot 10^{-8}$	$11.98 \cdot 10^{-8}$	$1.61 \cdot 10^{-8}$	$1.00 \cdot 10^{-7}$
32	$2.35 \cdot 10^{-8}$	$7.21 \cdot 10^{-8}$	$9.39 \cdot 10^{-9}$	$2.50 \cdot 10^{-8}$
42	$3.31 \cdot 10^{-8}$	$7.58 \cdot 10^{-8}$	$1.32 \cdot 10^{-8}$	$1.53 \cdot 10^{-8}$

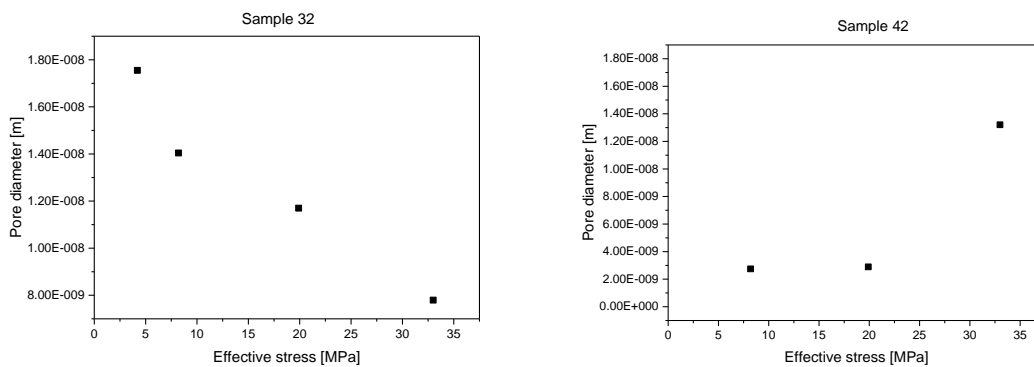


Figure 2. Pore diameter at different stress states presented for selected samples

Tests at different stress conditions were performed on samples 32 and 42; for sample 32, an increase in effective stress caused a decrease in effective pore size. Such a trend is very intuitive and is expected behavior of a reservoir during hydrocarbon production. However, for some samples increasing effective stress caused the opposite results, as shown in Fig.2 (sample 42). This is attributed to the fact that smaller pores, which are most responsible for

slippage, are cut off from the flow at high effective stress, therefore the slippage effect decreases and the effective pore size increases. A similar decrease in slippage was previously reported for Eagle Ford Shales.

In order to provide proper estimation of permeability in reservoir conditions, the effect of temperature needs to be taken into account. Temperature significantly affects gas density and the mean free path of gas molecules, thus resulting in lower permeability. For the tested samples, there was a change in permeability of one order of magnitude. Moreover, slippage is negatively correlated with permeability and, thus, significantly reduces estimated effective pore diameter.

CONCLUSION

In order to provide more accurate estimation of clay rich shale permeability, additional pore characterization using Klinkenberg slippage is needed on an existing well-characterized plug. Pore size distribution obtained by conventional analysis performed in unstressed conditions may lead to significant errors. However, as has been shown in the paper, microfractures may reduce the effect of stress in rocks with specific mineral composition and pore space structure; thus, dominant pore diameter might be included in estimations of permeability. Initially, it seemed that SEM image analysis produced similar pore diameter measurements as Klinkenberg slippage. However, more detailed analysis showed a large discrepancy between the results. Moreover, for production simulation, correction related to reservoir temperature needs to be considered (as with other reservoir conditions, temperature is naturally included in permeability Pulse Decay measurements).

ACKNOWLEDGEMENTS

This article is the result of research conducted as part of the project *Methodology of determining sweet spots on the basis of geochemical, petrophysical, and geomechanical properties, based on the correlation of the results of laboratory examinations with the geophysical measurements and the 3D generation model*, co-funded by the National Centre for Research and Development as part of the BLUE GAS – POLISH SHALE GAS program. Contract no. BG1/MWSSSG/13.

REFERENCES

1. Akkutlu I., Didar B., “Pore size dependence of fluid phase behaviour and properties in organic-rich shale reservoirs”, *SPE 1640099* SPE International Symposium on Oilfield chemistry, 8-10 April, The Woodlands, USA
2. Cui A., Wust R., Nassichuk B., Glover K., Brezovski R., Twemlow C., “A nearly complete characterization of permeability to hydrocarbon gas and liquid for unconventional reservoirs: a challenge to conventional thinking”, *SPE 168730*, Unconventional Resources Technology Conference, 12-14 August, Denver, USA
3. Heller R., Vermylen J., Zoback M., “Experimental investigation of matrix permeability of gas shales”, *AAPG Bulletin*, **98**, 975-995
4. Rydzy M., Patino J., Elmetni N., Appel M., “Stressed permeability in shales: effect of matrix compressibility and fractures – a step towards measuring matrix permeability in fractured shale samples”, *SCA2016-027*, 21-26 August, Snowmass, CO, USA